Eur. J. Mech. B/Fluids, **17**, n° 4, 595–604, 1998

Kelvin twist waves in the transition to turbulence

Steve ARENDT [a]*, David C. FRITTS [a], Øyvind ANDREASSEN [b]

ABSTRACT. – We present evidence for Kelvin twist waves on vortex tubes in a numerical simulation of the transition to turbulence in a breaking internal gravity wave. Specifically, $m = 0$, $m = 1$, and $m = 2$ twist waves are found and are compared to analytic versions of the waves. The observed twist waves are of a sufficiently large amplitude to break up the vortex tubes on which they reside, with the $m = 0$ waves fragmenting the vortex tubes along their length and the $m = 2$ waves unraveling the vortex tubes into pairs of helical tubes. Under the influence of these waves, the flow evolves from an organized collection of horseshoe vortices to a disorganized collection of vortex fragments. © Elsevier, Paris

1. Introduction

Recent numerical studies (Rogers and Moin 1987, Vincent and Meneguzzi 1991, 1994) have shown that vortex tubes, usually formed from the roll-up of vortex sheets, are ubiquitous in turbulent flows. One might even go so far as to say that vortex tubes comprise turbulence. As such, the dynamics of the turbulence are, in large part, controlled by the dynamics of the vortex tubes as they interact with any large-scale flow present, with their neighbors, and with themselves. In particular, recent work has shown that self-dynamics of vortex tubes in the form of waves on vortex tubes leads to the bursting of vortex tubes in numerical simulations of the transition to turbulence in a breaking gravity wave (Andreassen *et al.* 1998, Fritts *et al.* 1998). Similar events are visible in experimental results for turbulent shear flow (Cadot *et al.* 1995).

Waves on vortex tubes have a long history, beginning with Lord Kelvin (1880) who showed that the oscillation modes of a vortex tube of constant vorticity are stable. Subsequent authors have focussed on wavemodes for general core structures (Moore and Saffman 1972), on large-amplitude waves (Hasimoto 1972, Leibovich and Ma 1983, Leibovich *et al.*, 1986), and on the destabilization of wavemodes by straining and shearing flows (Moore and Saffman 1975, Tsai and Widnall 1976, Marshall and Chen 1997, Arendt and Fritts 1997). Several experimental studies (Hopfinger *et al.* 1982, Maxworthy *et al.* 1985) have shown that waves are easily excited on laboratory vortex tubes and that linear theory gives a reasonable prediction for their properties. The excitation of twist waves from the initial state of a vortex tube has been recently studied (Arendt *et al.* 1997), while the core dynamics of a vortex tube, which are related to twist waves, have been studied for an initial perturbation of a vortex tube (Melanger and Hussain 1994) and for the forcing of a tube by an external flow (Verzicco *et al.*, 1995).

The present paper focuses on the vortex wave events found numerically by Fritts *et al.* (1998) in the transition to turbulence in a breaking internal gravity wave. We provide a comparison of those events with linear Kelvin vortex-wave theory, emphasizing the similarity in the form of the waves and the physics providing for the wave's propagation. Section 2 provides a brief introduction to the breaking internal gravity wave studied, while the remainder of the paper is divided into sections by the azimuthal wavenumber of the wave events, with $m = 0$, $m = 1$, and $m = 2$ events being presented in Sections 3, 4, and 5, respectively.

[a] Colorado Research Associates/NWRA, 3380 Mitchell Lane, Boulder, CO 80301, USA
[b] Norwegian Defence Research Establishment, Kjeller, Norway
* Correspondence and reprints

0997-7546/98/04/© Elsevier, Paris

2. The breaking internal gravity wave event

We begin with a brief description of the gravity wave breaking event leading to the transition to turbulence. We will describe only the flow evolution; details of the numerical method may be found in the references (Fritts *et al.*, 1998; Andreassen *et al.*, 1998). In our numerical simulations, an internal gravity wave propagates into a critical layer formed by a shear flow. Plate 1 shows the evolution of a single isosurface of potential temperature chosen to display the overturning of the wavefront as the wave breaks. The times shown are $t = 62.5, 65.0, 67.5,$ and 70.0, and are normalized by the sound crossing time of a density scale height. To put these times in perspective, a buoyancy period is 14.0 in these normalized units, so that Plate 1 shows somewhat less than a full buoyancy period. The wave propagates horizontally to the right (and slightly vertically) in Plate 1; we will call this direction the streamwise direction, and we will call the orthogonal horizontal direction the spanwise direction. The computational domain is periodic in the streamwise direction, so that as the wave exits the right side of the domain, it re-enters the left side. Prior to the times shown in Plate 1, the internal gravity wave was a linear wave of small amplitude. By $t = 60$, the wave has propagated vertically into a shear flow whose flow velocity is in the streamwise direction and whose vorticity is in the spanwise direction. This shear causes the wavefronts to steepen and overturn as seen in Plate 1. The overturned flow is convectively unstable, leading to convective rolls whose axes are streamwise; the rolls can be seen in Plate 4 of Fritts *et al.* (1994). The fluid collapses in these rolls, causing the corrugation of the wavefront seen in Plate 1 at $t = 62.5$ and $t = 65.0$ as well as the chaotically mixed region on the left side of the computational domain at $t = 70.0$. This region will be of interest for the transition to turbulence study in the following section.

Plate 1. – An isosurface of potential temperature for the gravity wave breaking simulation, viewed at an angle with positive x (streamwise) to the right. Times $t = 65$, 70, 75, and 80 are shown. The form of the overturning wave front is clearly visible.

In addition to mixing the convectively unstable fluid, the flow of the streamwise convective rolls affects the spanwise vorticity of the background shear. This spanwise vorticity is initially horizontally uniform over the computational domain, but as time proceeds it is stretched and amplified whenever the convective flow diverges in the spanwise direction. The result is a collection of local intense vortex sheets marking the locations of divergent convective flow (as can be seen in Plate 2 of Andreassen *et al.*, 1998). The sheets are curved from the flow of the convective rolls, and are finite in extent in all three directions, having streamwise widths of roughly 10-20 sheet thicknesses and spanwise widths of roughly 6 sheet thicknesses. The sheets are sufficienlty thin and intense to undergo the Kelvin-Helmholtz instability which rolls each sheet up into 3-4 parallel vortex tubes. The tubes are curved from the original curvature of the sheets, and the background shear flow stretches and rotates

the tubes until the flow in the unstable phase of the wave becomes a collection of intertwined vortex loops, closely resembling the horseshoe vortices arising in turbulent boundary layer flows (Acarlar and Smith, 1987; Robinson, 1991; Sandham and Kleiser, 1992) or in sheared turbulence (Gerz *et al.*, 1994). These horseshoe vortices are seen at $t = 70$ in Plate 2, wich displays the vortex cores in the entire computational domain traced out in the λ_2 eigenvalue of Jeong and Hussain (1995). Times $t = 65$, 70, 75, and 80 are shown and the view is from below, with streamwise to the right and spanwise upward.

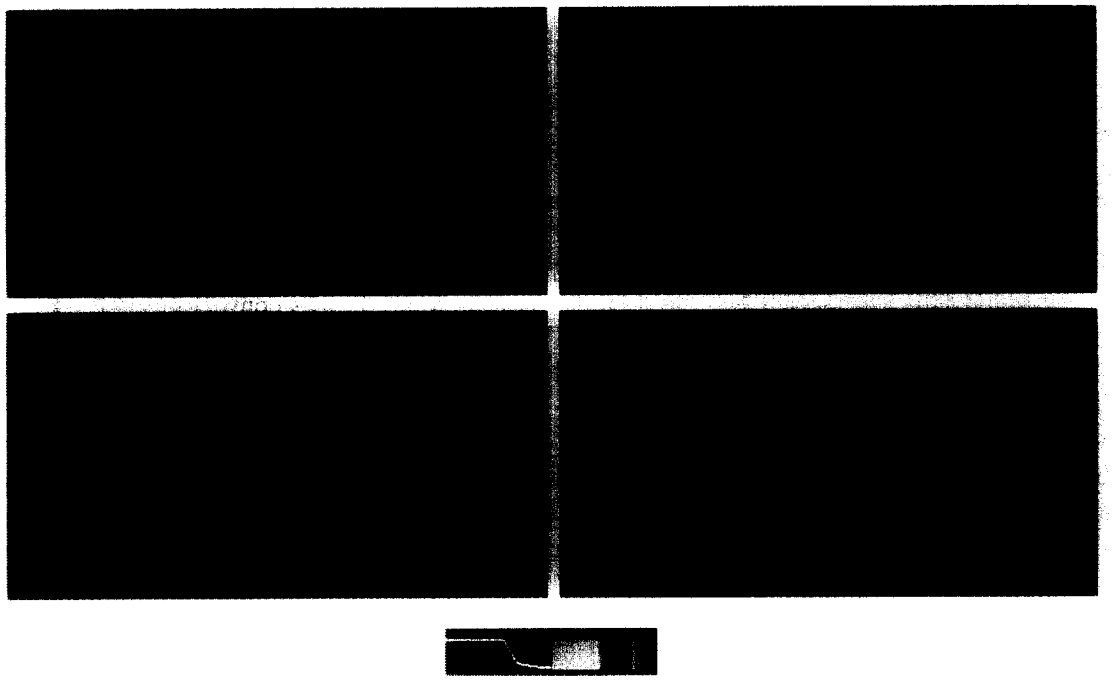

Plate 2. – Volume renderings of λ_2 for the gravity wave breaking simulation viewed from below with positive x (streamwise) to the right. Times $t = 65$, 70, 75, and 80 are shown.

Consider the evolution of the vortex cores shown in Plate 2. The streamwise vortices shown at $t = 65$ are the streamwise convective rolls mentioned above. As time proceeds, curved spanwise vortices (horseshoe vortices) appear, having been formed from the roll-up of spanwise vortex sheets [†]; three of these appear in the upper left corner of the $t = 65$ panel. By $t = 70.0$, many horseshoe vortices are present; these vortices occupy a thin approximately-horizontal layer of the domain where the gravity wave is unstable. At $t = 75.0$, still more vortices have formed, and some horseshoe vortices are beginning to become fragmented. The fragmentation takes place on a vortex circulation timescale, $\tau = 4\pi/\omega$, which is roughly 2.0 in normalized units. The fragmentation is caused by large-amplitude vortex waves that are excited on the vortex tubes; this will be shown in the following sections where we examine in detail individual vortex tubes undergoing fragmentation. Finally, at $t = 80.0$ essentially all the horseshoe vortices have been fragmented.

[†] The vortex sheets are not shown in Plate 2 because of the nature of the λ_2 eigenvalue used for the display; only vortices whose local flow is roughly rotational are shown (Jeong and Hussain, 1995).

3. Kelvin twist waves with $m = 0$

We begin with a short review of Kelvin waves (Kelvin, 1880), or alternatively twist waves, on a vortex tube. If one linearizes the Euler equations around a base state consisting of a straight vortex tube with constant vorticity, the equations admit wave modes having an axial velocity

$$u_z^i(r, \phi, z) = C \frac{J_m(k\xi_n r)}{J_m(k\xi_n a)} e^{i(m\phi+\omega_n t-kz)}, \tag{3.1}$$

$$u_z^o(r, \phi, z) = C \frac{K_m(kr)}{K_m(ka)} e^{i(m\phi+\omega_n t-kz)}, \tag{3.2}$$

where C is a constant amplitude, and where the quantity ξ is given by

$$\xi_n^2 = \frac{4\Omega^2}{(\omega_n + m\Omega)^2} - 1. \tag{3.3}$$

We give only the form of the axial flow as this is the most convenient component; the other flow components are easily found from the Euler equations (see e.g. Arendt *et al.*, 1997). The integer m is the azimuthal wavenumber of the mode. The perturbation of a vortex tube by a single wavemode takes the form of m helices. The subscript n is the radial number of the mode; modes with higher n have more complicated radial structure than those with lower n. The dispersion relation is found to be

$$\frac{J'_m(k\xi_n a)}{k\xi_n a J_m(k\xi_n a)} + \frac{2m\Omega}{(k\xi_n a)^2(\omega_n + m\Omega)} + \frac{K'_m(ka)}{kaK_m(ka)} = 0, \tag{3.4}$$

all of whose solutions ω_n are real so that the Kelvin wavemodes are all stable propagating waves.

Consider an $m = 0$ Klevin wavemode. Such a wave propagates by alternately twisting and untwisting the vortex lines comprising the vortex tube. The $\hat{\phi}$ component of the vorticity in the twisted lines induces a flow along the axis of the vortex tube. This axial flow, u_z, stretches (amplifies) the axial vorticity where the flow diverges, and scrunches (depletes) it where the flow converges. This change in axial vorticity changes the rotational velocity, u_ϕ, of the vortex tube's flow; an increase in the axial vorticity increases u_ϕ, while a decrease in the axial vorticity decreases u_ϕ. This change in u_ϕ twists/untwists the vortex lines and the process repeats. The key feature of an $m = 0$ twist wave, then, is a twisting of a tube's vortex lines and a consequent axial flow.

We have identified many examples of $m = 0$ twist waves in our gravity wave breaking simulation, one of which is shown in the upper row of panels in Plate 3. Here a spanwise vortex tube is shown in λ_2 at times $t = 70.5$, 71.5, 72.5, and 73.5. Also shown are smaller orthogonal vortex tubes near the top and bottom of the spanwise tube; these are the legs of a horseshoe vortex lying just upstream of the present vortex tube. At $t = 70.5$, the vortex tube is just forming from the roll-up of a vortex sheet. As time proceeds, the tube initially becomes stronger ($t = 71.5$), but then grows weaker first near the top of the tube ($t = 72.5$), and then in the center of the tube ($t = 73.5$). The depletion in the center of the tube irreversibly fragments the tube into two pieces.

The depletion of the tube is the result of $m = 0$ twist wave propagation. To see this, consider the upper row of panels of Plate 4 which show vortex lines (in yellow) and isosurfaces of axial flow (with red positive and blue negative). Vorticity vectors are also shown in white; the vorticity of the tube points downward in Plate 4. At $t = 70.5$, the vortex tube is not quite formed, but one can see from the curved path of the vortex lines that the top of the tube is rolling up faster than the middle. By $t = 71.5$, the tube is well-formed, and its vortex

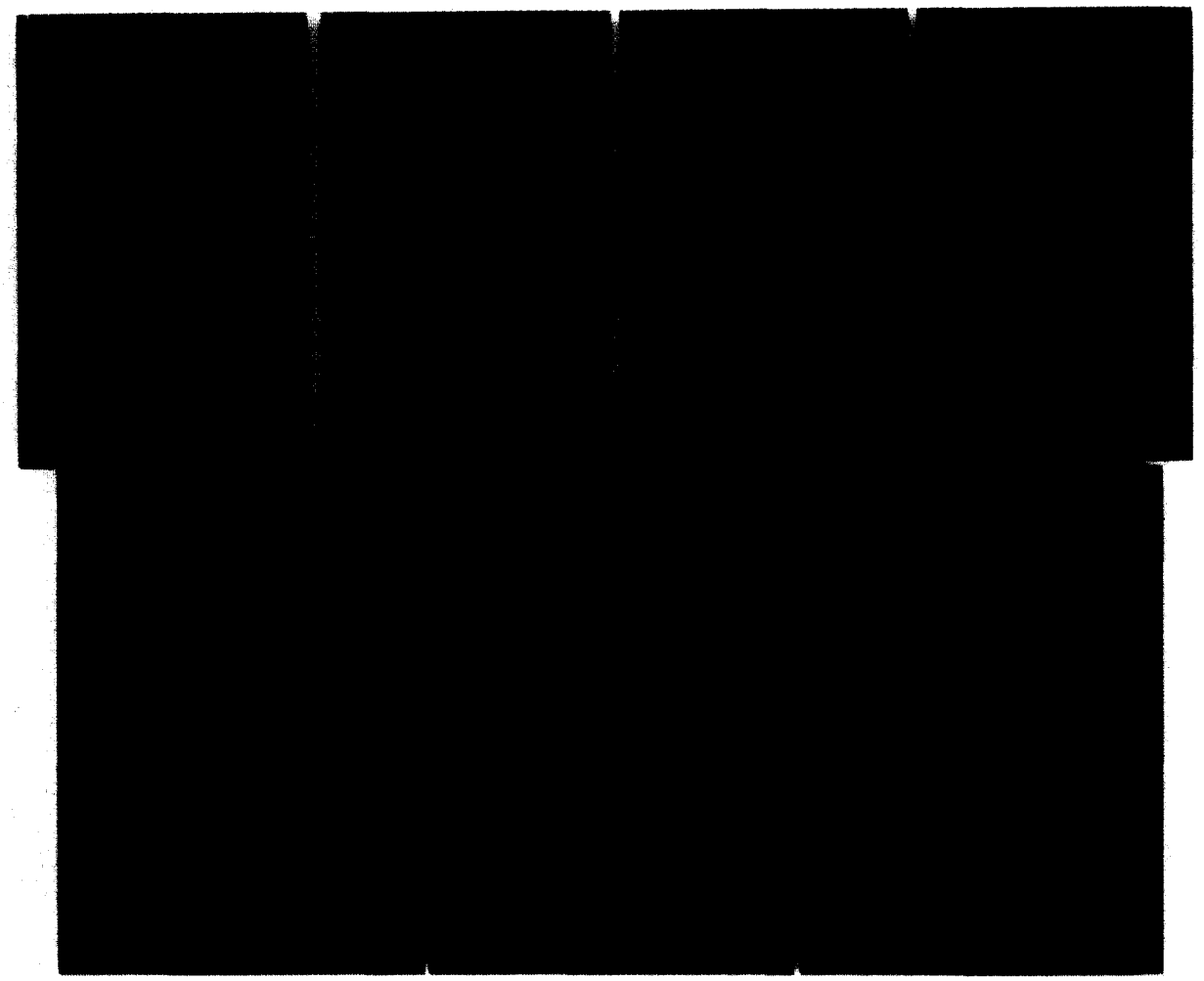

Plate 3. – Volume renderings of λ_2 for two twist wave events in the gravity wave breaking simulation. The top panels show an $m = 0$ wave at $t = 70.5$, 71.5, 72.5, and 73.5. The bottom panels show an $m = 1$ wave at $t = 71$, 72, and 73.

lines have retained the twist they acquired during the roll-up, i.e., they are twisted so that there is a positive ω_ϕ (if we define $\hat{z}$ as being upward in Plate 4 so that $\omega_z < 0$). This ω_ϕ induces an axial flow upward ($u_z > 0$) in the tube which is shown by the red isosurface within the tube. The axial flow strengthens the vorticity in the middle of the tube which in turn increases the rotational velocity in the middle of the tube. This increased rotational velocity untwists the original twist given to the tube and twists the tube up in the opposite sense after half of a vortex circulation time (recall that the vortex circulation time is roughly 2.0 in these units), as is seen at $t = 72.5$. This opposite twist induces an opposite axial flow, as shown by the blue isosurface ($u_z < 0$) within the tube at $t = 72.5$. In addition to the downward axial flow at the top of the tube, the twist induces an upward axial flow at the bottom of the tube (see the red isosurface within the tube at $t = 72.5$). These axial flows converge at the middle of the tube, weakening the vorticity there, increasing the radius, and causing the depletion of the middle of the vortex tube as noted in Plate 3.

For comparison, the lower panels of Plate 4 show the results of an analytic solution of the linearized initial value problem for a tube of constant vorticity (Arendt *et al.*, 1997). Of course, the vortex tubes in the wave-breaking simulation do not have constant vorticity, but these analytic results still provide a useful comparison

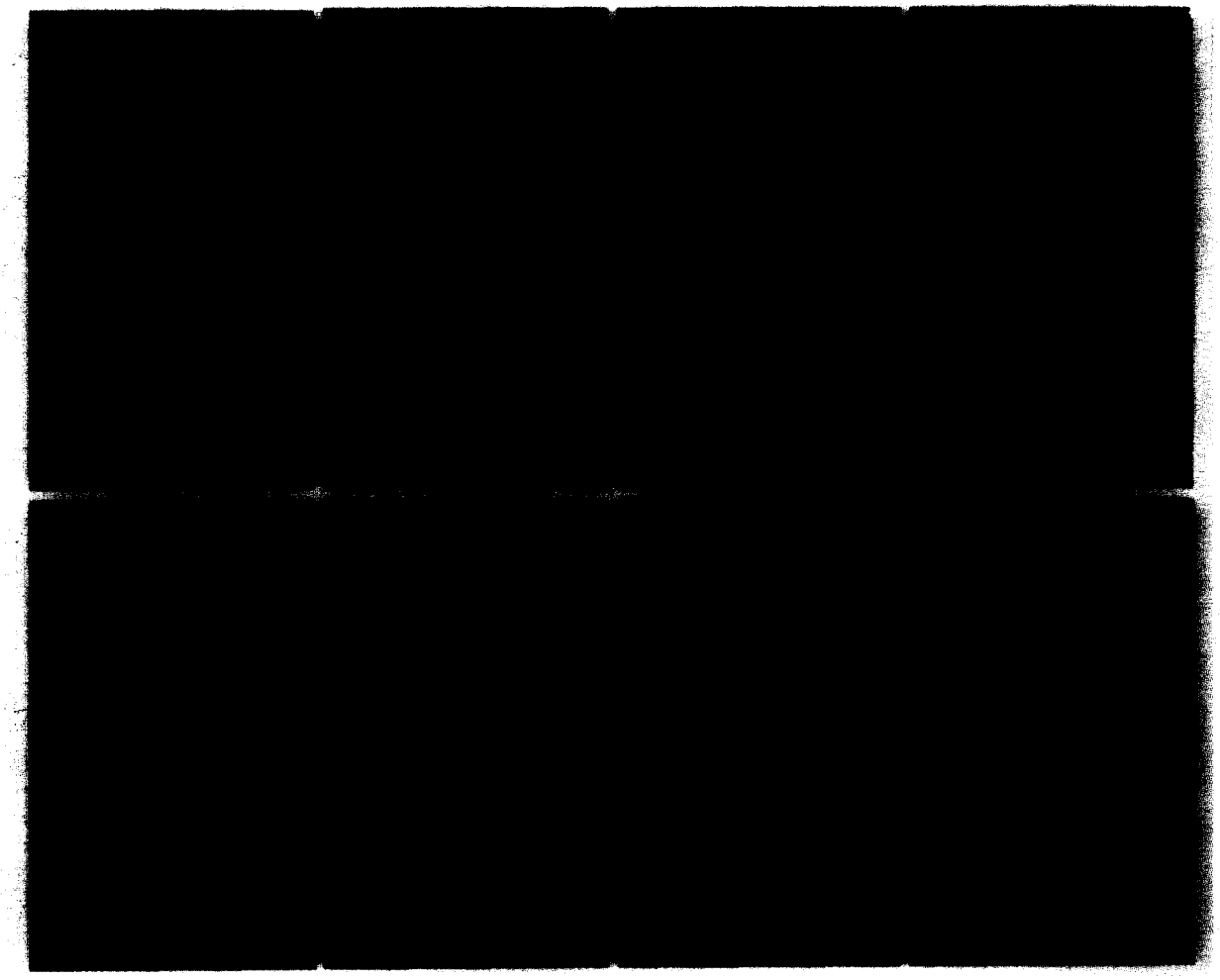

Plate 4. – Vortex lines and isosurfaces on axial flow velocity for $m = 0$ twist wave packets. The upper panels show the same event and timesteps as in the upper panels of Plate 2; the isosurface magnitudes are ± 0.05 with red positive and blue negative, except at $t = 71.5$ for which the isosurface magnitudes are ± 0.03. The lower panels show an analytic example at times $t = 0.0$, 0.5, 1.0, and 1.5; the isosurface magnitudes are ± 0.10 at $t = 0.5$, ± 0.05 at $t = 1.0$, and ± 0.04 at $t = 1.5$.

because the physics of the twist waves is robust and does not depend on the detailed vorticity distribution of the tube. Times $t = 0.0$, 0.5, 1.0, and 1.5 are shown, with the time normalized by the circulation time of the vortex. The perturbation to the tube is given a large amplitude for display, even though the calculation is linear. The tube is initiated with a weaker vorticity in the middle compared to the top and bottom. This causes the ends of the tube to rotate faster than the middle, as occurs in the first panel in the upper row of panels in Plate 4. The faster rotation twists the vortex lines (which are initially untwisted) in the same sense as occurs in the wave breaking case, inducing an axial flow which diverges in the center of the tube (see $t = 0.5$). The diverging flow amplifies the vorticity in the middle of the tube, increasing the flow rotation and twisting the vortex lines in the opposite sense (see $t = 1.0$). This reverses the axial flow (except at the very ends of the tube), so that the flow now converges at the center of the tube. The timescale for the twist to reverse is the same as for the wave-breaking simulation: half of a vortex circulation time (recall that a circulation time is 1.0 for the analytic calculation).

At later times (see $t = 1.5$), the amplitude of the axial flow has decreased so that the tube does not undergo fragmentation. This is due to the fact that the analytic calculation is linear so that the initial perturbation

decomposes entirely into linear Kelvin waves which propagate away from the site of the initial perturbation. Since linear Kelvin waves are stable, they cannot fragment the tube. On the other hand, in the gravity wave breaking simulation, the twist waves are excited with too large amplitude to be considered linear (see e.g. $t = 72.5$), and so they subsequently amplify and fragment the tube ($t = 73.5$).

4. Kelvin twist waves with $m = 1$

An $m = 1$ twist wave displaces the center of the vortex tube into a helix. The source of the wave's propagation is the curvature self-advection of the vortex tube; a curved vortex tube advects itself in a direction orthogonal to both the tube and the radius of curvature. The curvature self-advection of a helical vortex tube has both an axial component and an azimuthal component, so that the wave has both an axial propagation as well as an azimuthal rotation.

The lower panels of Plate 3 show an example of an $m = 1$ twist wave at times $t = 71$, 72, and 73 in the gravity wave breaking simulations. At $t = 71$, the long curved vortex tube has a smaller orthogonal vortex tube lying very close to it near its lower end. The flow of this orthogonal tube perturbs the longer tube (and vice versa) deflecting it slightly from its original location (see the bump in the tube at $t = 72$). However, deflecting a vortex tube in this fashion excites $m = 1$ twist waves via the curvature self-advection, so that the initial deflection becomes a helix ($t = 73$). Unlike the $m = 0$ and $m = 2$ twist waves present in our simulation, the $m = 1$ waves do not amplify, and so do not lead to fragmentation or bursting; at later times, the $m = 1$ wave in Plate 3 is the same as in the last panel of Plate 3.

Surprisingly, the helical wave in Plate 3 does not appear to propagate or rotate. Now, there do exist $m = 1$ wavemodes which do not propagate (see, e.g., Saffman, 1992), but those modes have considerable radial structure which the non-propagating wave in Plate 4 does not have. A possible explanation for the lack of propagation is that the wave in Plate 3 is being continuously forced by the flow of the neighboring orthogonal vortex, and since the forcing is always at the same location on the vortex tube, the phase of the excited $m = 1$ wave is also always at the same location.

5. Kelvin twist waves with $m = 2$

Twist waves with $m = 2$ are very common in our gravity wave breaking simulations, and cause vortex tubes to unravel into pairs of intertwined helices. The upper row of panels in Plate 5 shows an example from our simulations at times $t = 72$, 73, 74, 75, and 76. Here, volume rendering is used to display the λ_2 eigenvalue. The wave propagates downward in the Plate (this is the positive streamwise direction in the simulation), but the frame is moved over time to track the propagating wave packet. The $m = 2$ wave in Plate 5 is initially of small amplitude and grows to an amplitude sufficient to split the vortex tube into two intertwined helices. As the circulation time is approximately 2.0, we see that the wave amplification takes about one circulation time. Although it is difficult to see in the Plate, the double helix pattern rotates, completing half of a revolution from $t = 74$ to $t = 76$. Another example of an $m = 2$ wave appears in the upper panels of Plates 3 and 4; here an $m = 2$ wave unravels the bottom end of the horseshoe vortex shown.

Consider the physics of an $m = 2$ wave's propagation. As in the case for the $m = 1$ wave, the $m = 2$ wave is propelled by self-advection; that is, its own velocity field advects it along. In the case of the wave packet shown, the helical vortex lines induce both an azimuthal and an axial flow; the latter accounts for the axial propagation of the wave packet, while the former accounts for the rotation of the double-helix pattern around the tube. The sense of the helices and the direction of the vorticity determine the direction of the axial velocity

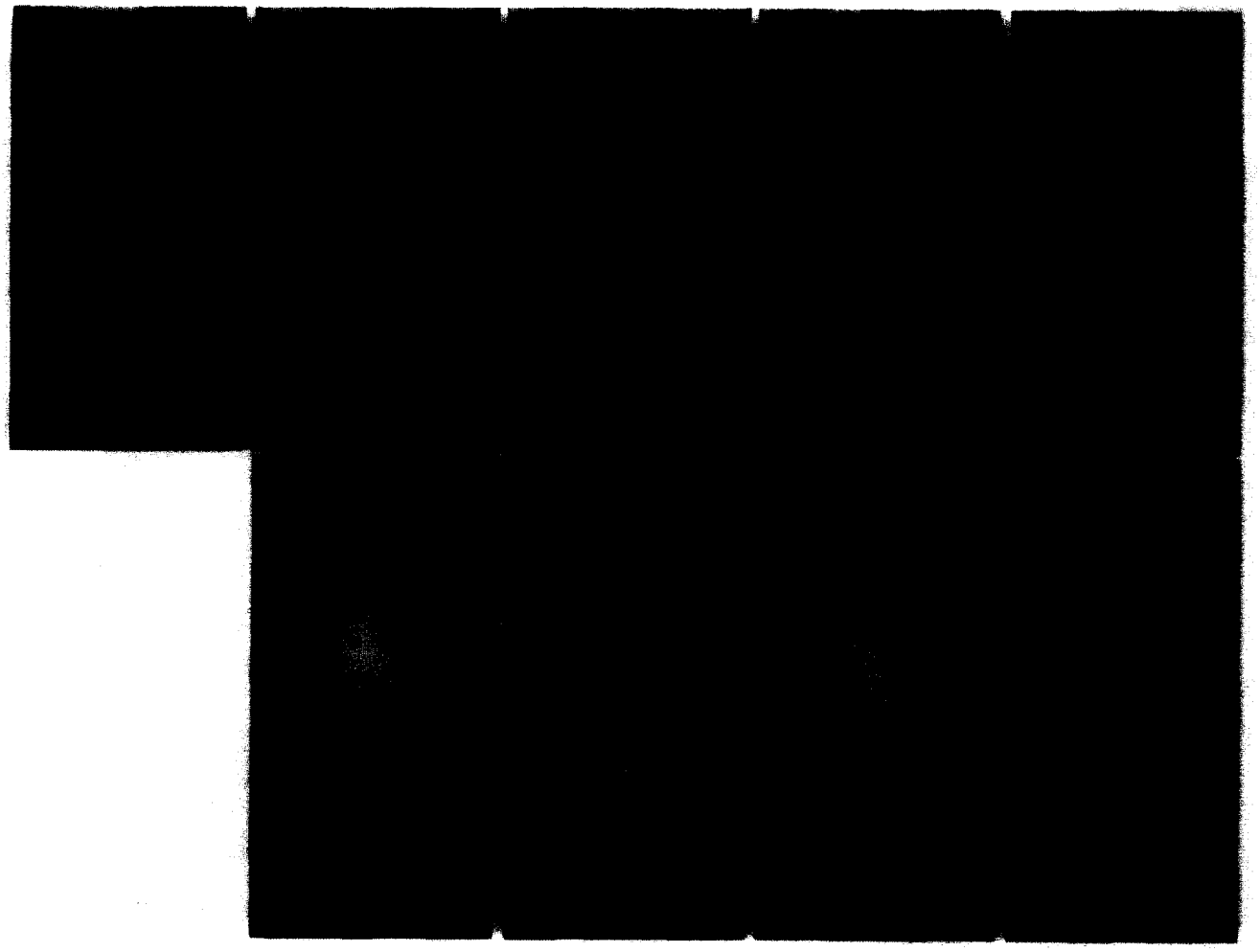

Plate 5. – The top panels show volume renderings of λ_2 for an $m = 2$ wave event in the gravity wave breaking simulation at $t = 72$, 73, 74, 75, and 76. The bottom panels show the surface of a vortex tube for an analytic example of an $m = 2$ wave packet at $t = 4.5$, 5.0, 5.5, and 6.0.

and, hence, the direction of the wave's propagation. Just in front of the wave packet in Plate 5, the vorticity lines induce a diverging radial flow which splits the tube into the two helical components, so that the wave packet can propagate into undisturbed regions of the vortex tube.

The lower row of panels in Plate 5 shows an analytic example of an $m = 2$ twist wave packet. In this case, an initial flattening of a vortex tube's cross-section produces two $m = 2$ wave packets, each with a different sense of helicity propagating in different directions away from the site of the original perturbation (see Arendt *et al.* 1997 for a complete description). In Plate 5, we show one of the wave packets propagating downward at $t = 4.5$, 5.0, 5.5, and 6.0 with the times normalized by the vortex circulation time $\tau = 4\pi/\omega$. The calculation of the evolution is linearized, but the amplitude of the wave is made large intentionally for display. In this example, we see the same double helix form as in the simulation example. Also, the wave packet's axial propagation and azimuthal rotation are clearly seen. The rotation takes one circulation time for half a rotation, in agreement with the example from the wave-breaking simulation. As in the case of the $m = 0$ wave, the linearized analytic calculation does not allow the wave to split the vortex tube into two helical tubes.

6. Discussion

In this paper, we study the vortex tube dynamics within the transition to turbulence in a numerical simulation of a breaking gravity wave. During its initial evolution, the wave undergoes both a convective instability and a shear (Kelvin-Helmholtz) instability that concentrates the vorticity of the flow into a collection of horseshoe vortices. At later times, Kelvin vortex waves, or twist waves, are excited on the horseshoe vortices, and these serve to fragment, unravel, and burst the vortices. At must later times, all the horseshoe vortices are split into pieces, and essentially all of this splitting can be traced back to twist waves. At this stage in the flow's evolution, then, twist waves appear to be the dominant mechanism for transferring energy to smaller scales and for homogenizing and isotropizing the flow.

The twist waves in our simulation are excited primarily by the initial state of the tube, which is dictated by the form of the roll-up of the vortex sheets undergoing shear instability. Since the vortex sheets are finite in extent rather than infinite, the resulting tubes are finite in extend, and so have variations in structure along their axes. These variations excite twist waves as the vortex tube tries to adjust itself toward axial uniformity. Twist waves with $m = 0$ and $m = 2$ are the most common ones excited in this way, and also are the most destructive to the tubes. Twist waves may also be excited on a vortex tube by an interaction with a neighboring tube, as in the case of the $m = 1$ example discussed in Section 3.

To consider the excitation in more detail, twist waves with $m = 0$ are excited on a vortex tube where one portion of the tube is more intense (i.e., has higher vorticity) and rolls up faster than the other portions of the tube. This is common since finite vortex sheets are typically more intense in their middles than at their ends, so the resulting vortex tubes are also typically more intense in their middles. The faster roll-up twists the vortex lines, which in turn induce axial flows along the tube. These axial flows lead to the destruction of the portion of the vortex tube where the flow converges, hence fragmenting the tube.

It often happens that the ends of a vortex tube are initially not axisymmetric, but are rather slightly split in two. If we view the roll-up of a vortex sheet as coalescing the vortex lines of the sheet into a tube, then the lines that are gathered from one side of the tube and those that are gathered from the other side form two distinct groups. In the bulk of the tube, the lines of these two groups meld together, but at the ends of the tube, the lines of the two groups go off in different directions and maintain their connectivity with the rest of the flow. This splits the end of the tube in two, which in turn excites an $m = 2$ twist wave propagating inward along the tube and unraveling the tube into a pair of intertwined helices, as seen in Plate 5.

Vortex tubes are ubiquitous in turbulent flows and in flow undergoing the transition to turbulence. These tubes are finite in length and are usually formed by the roll-up of finite-extent vortex sheets. As such, the tubes should be susceptible to twist wave excitation, and possibly also to fragmentation and unraveling. Twist waves on vortex tubes may thus be an important dynamical mechanism in general for the transfer of energy to smaller scales in a fully turbulent flow or in a flow transitioning to turbulence.

Support for this work was provided by the Norwegian Defence Research Establishment, the National Science Foundation under grants ATM-9419151 and ATM-9618004, and the Air Force Office of Scientific Research under grants F49620-95-1-0286 and F49620-96-1-0300.

REFERENCES

ACARLAR M. S., SMITH C. R., 1987, A study of hairpin vortices in a laminar boundary layer. Part II: Hairpin vortices generated by fluid injection, *J. Fluid Mech.*, **175**, 43-83.

ANDREASSEN Ø., HVIDTEN P. Ø., FRITTS D. C., ARENDT S., 1998, Vorticity dynamics in a breaking gravity wave 1: Initial instability evolution, *J. Fluid Mech.*, accepted.

ARENDT S., FRITTS D. C., ANDREASSEN Ø., 1997, The initial value problem for Kelvin vortex waves, *J. Fluid Mech.*, **344**, 181-212.

ARENDT S., FRITTS D. C., 1997, The instability of a vortex tube in a weak external shear and strain, *Phys. Fluids A*, **10**, 530-532.

CADOT O., DOUADY S., COUDER Y., 1995, Characterization of the low-pressure filaments in a three-dimensional turbulent shear flow, *Phys. Fluids A*, **7**, 630.

FRITTS D. C., ISLER J., ANDREASSEN Ø., 1994, Gravity wave breaking in two and three dimensions 2. Three-dimensional evolution and instability structure, *J. Geophys. Res.*, **99**, 8109-8123.

FRITTS D. C., ARENDT S., ANDREASSEN Ø., 1998, Vorticity dynamics in a breaking gravity wave 2: Vortex interactions and transition to turbulence, *J. Fluid Mech.*, accepted.

GERZ T., HOWELL J., MAHRT L., 1994, Vortex structures and microfronts, *Phys. Fluids A*, **6**, 1242-1251.

HASIMOTO H., 1972, A soliton on a vortex filament, *J. Fluid Mech.*, **51**, 477-485.

HOPFINGER E. J., BROWAND F. K., GAGNE Y., 1982, Turbulence and waves in a rotating tank, *J. Fluid Mech.*, **125**, 505-534.

JEONG J., HUSSAIN F., 1995, On the identification of a vortex, *J. Fluid Mech.*, **285**, 69-94.

LEIBOVICH S., BROWN S. N., PATEL Y., 1986, Bending waves on inviscid columnar vortices, *J. Fluid Mech.*, 595-624.

LEIBOVICH S., MA H. Y., 1983, Soliton propagation on vortex cores and the Hasimoto soliton, *Phys. Fluids*, **26** 3173-3179.

Lord KELVIN, 1880, Vibrations of a columnar vortex, *Phil. Mag.*, **10**, 155.

MARSHALL J. S., CHEN H., 1997, Stability of a counter-rotating vortex pair immersed in cross-stream shear flow, *AIAA Journal*, **35**, 295.

MAXWORTHY T., HOPFINGER E. J., REDEKOPP L. G., 1985, Wave motions on vortex cores, *J. Fluid Mech.*, **151**, 141-165.

MELANDER M. V., HUSSAIN F., 1994, Core dynamics on a vortex column, *Fluid Dyn. Res.*, **13**, 1-37.

MOORE D. W., SAFFMAN P. G., 1972, The motion of a vortex filament with axial flow, *Phil. Trans. Royal Soc. A*, **272**, 403-429.

MOORE D. W., SAFFMAN P. G., 1975, The instability of a straight vortex filament in a strain field, *Proc. R. Soc. Lond. A*, **346**, 413-425.

ROBINSON S. K., 1991, Coherent motions in the turbulent boundary layer, *Annu. Rev. Fluid Mech.*, **23**, 601-639.

ROGERS M. M., MOIN P., 1987, The structure of the vorticity field in homogeneous turbulent flows, *J. Fluid Mech.*, **176**, 33.

SAFFMAN P. G., 1992, *Vortex Dynamics*, Cambridge University Press.

TSAI C.-Y., WIDNALL S. E., 1976, The stability of short waves on a straight vortex filament in a weak externally imposed strain field, *J. Fluid Mech.*, **73**, 721-733.

VERZICCO R., JIMÉNEZ J., ORLANDI, P., 1995, On steady columnar vortices under local compression, *J. FLuid Mech.*, **299**, 367-388.

VINCENT A., MENEGUZZI, M., 1991, The spatial structure and statistical properties of homogeneous turbulence, *J. Fluid Mech.*, **225**, 1-20.

VINCENT A., MENEGUZZI M., 1994, The dynamics of vorticity tubes in homogeneous turbulence, *J. Fluid Mech.*, **258**, 245.

(Received 31 July 1997,
revised 14 November 1997,
accepted 9 January 1998)